Design Options for Stellarator Divertors

Alkesh Punjabi[1], Allen Boozer[2]

[1]Hampton University, Hampton, VA 23668, USA

[2]Columbia University, New York, NY 10227, USA

ABSTRACT: Divertors are thought to be required to concentrate the plasma particle exhaust region on the walls for effective pumping while avoiding plasma degradation by impurities from the walls. Concentration eases particle handling but makes power handling impossible unless the power exhaust can be spread by electromagnetic radiation or by the geometry of the interception region with the walls. What is possible with divertors is determined by (1) the relative shape of the wall and the plasma and (2) the topological nature of the magnetic field lines near the plasma edge—magnetic surfaces, islands or stochastic regions. The range of possible topologies can be efficiently represented by parameters in magnetic field line maps. The range of shapes of the walls and plasma can be given as parametric functions. Using parameterizations of the topology and shape, the design options for stellarator divertors are being studied along with their sensitivity to the rotational transform and its shear. This work is supported by the US DOE grants DE-FG02-01ER54624 and DE-FG02-04ER54793 to Hampton University and DE-FG02-95ER54333 to Columbia University.

Generally, there are two design options for stellarator divertor designs. The first, dominated by magnetic islands as on W7-X, and second dominated by stochasticity as on LHD [1]. The two designs are based on different principles: islands on the plasma surface for W7-X, called a resonant divertor, and the use of sharp edges on the quasiaxisymmetric stellarator, called the nonresonant divertor. Primary purpose of a divertor is to concentrate the region on the wall in which the plasma particle exhaust occurs so pumps can be installed at this location. Covering the whole wall with pumps is not practical. Concentrating the particle exhaust is advantageous; concentrating the plasma energy exhaust is not. A fifth of the power released by DT fusion is released in alpha particles that heat the plasma and the rest in neutrons, which directly heat the walls. If none of the alpha power were lost from the plasma by electromagnetic radiation roughly 20% of the wall area would need to be devoted to the divertor region in order to handle the power exhaust. This area could be in a volume through which the plasma has access by a slot, which gives what is called a closed divertor. Generally it is assumed that most of the power can be radiated. Radiated power may become sufficiently

large that the plasma recombines before it has contact with the surrounding structures. This is called plasma detachment. This gives a detached divertor. Some desirable features are: (1) a significant spatial separation between the region of good plasma containment and the intersection location of divertor field lines on the surrounding structures. This separation makes it more difficult of sputtered particles to enter the plasma volume. (2) A stable location for a slot for field lines to pass into a divertor chamber independent of the plasma state. (3) A controlled spreading of the heat load. The Hamiltonian equations for the field line are $d\psi_t/d\varphi = -\partial\psi_p/\partial\theta$ and $d\theta/d\varphi = \partial\psi_p/\partial\psi_t$. Position vector for field lines is given by $\vec{x}(\psi_t,\theta,\varphi) = R(\psi_t,\theta,\varphi)\hat{R}(\varphi) + Z(\psi_t,\theta,\varphi)\hat{Z}$. The standard position vector is given by $R = R_a(\varphi) + a\sqrt{\psi_t/\psi_a}\cos\theta, Z = Z_a(\varphi) + a\sqrt{\psi_t/\psi_a}\sin\theta.$ Here we investigate the resonant divertor design option for stellarators. We use the NCSX parameters [2]. The total Hamiltonian is $\psi_p(\psi_t,\theta,\varphi) = \overline{\psi}_p(\psi_t) + \widetilde{\psi}_p(\theta,\varphi)$. The unperturbed Hamiltonian is $\overline{\psi}_P(\psi_t) = a\psi_t + b\psi_t^2$. The perturbation is $\widetilde{\psi}_P(\theta,\varphi) = \delta\left[\cos(m_1\theta - n_1\varphi) + \cos(m_2\theta - n_2\varphi)\right]$. The resonant map equations are $\psi_{j+1} = \psi_j + k\delta[\sin(m_1\theta_j - n_1\varphi_j) + \sin(m_2\theta_j - n_2\varphi_j)]$, and $\theta_{j+1} = \theta_j + k\bar{\iota}(\psi_{j+1})$. Both forward and the backward map are used. Resonant perturbation have modes (2,1)+(5,3) with amplitude = 10^{-3}. Both modes are locked with no radial dependence. Footprints are calculated using continuous analogs of forward and backward maps. Lengths of lines, Liapunov lengths, and footprints are calculated. Two topologies for collecting surfaces; conformal tori and cylinders are studied. Here the tori are considered. The starting surface is shown in Fig. 4.

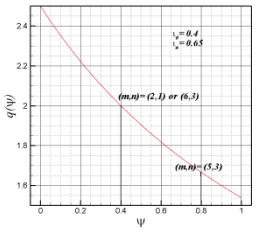

Fig. 1. Equilibrium safety factor for the NCSX.

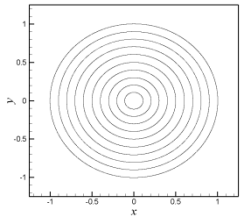

Fig. 2. The equilibrium magnetic surfaces in the NCSX generated by the map.

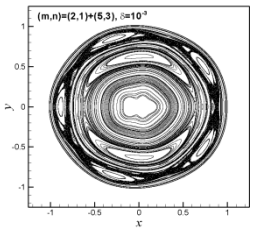

Fig. 3. Phase portrait for the resonant perturbation $(m,n)=(2,1)+(5,3)$ with the amplitude $\delta=10^{-3}$ in the $\varphi=0$ plane.

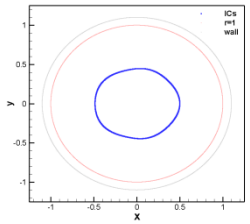

Fig. 4. The $r=1/2$ perturbed surface, the plasma boundary at minor radius $r=1$, and the wall at $r=1.1$ in the $\varphi=0$ plane.

The radially outward diffusion of field lines is implemented by the spiraling operator $r_{j+1} \rightarrow (0.9+0.2R_N D/N_p)r_{j+1}$. Phase portrait of starting surface from spiraling are shown in Fig. 5. The half-life, 1/e loss time, and the full confinement time all scale roughly as $1/D$.

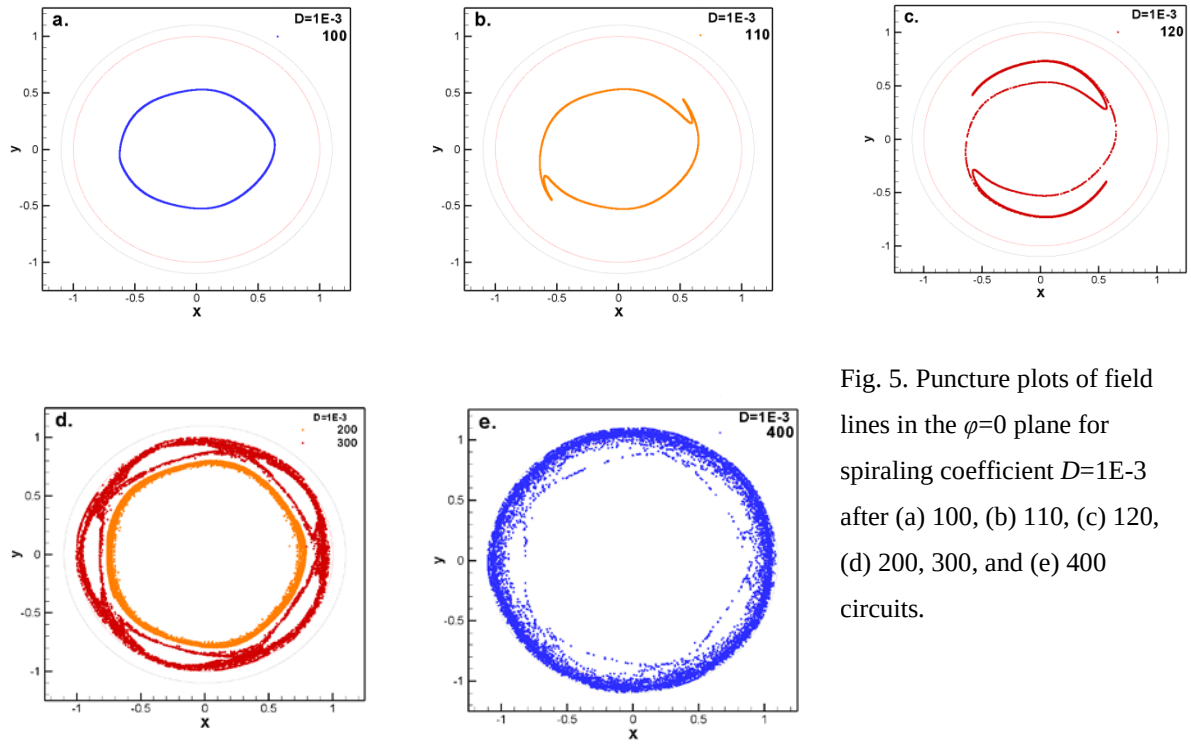

Fig. 5. Puncture plots of field lines in the φ=0 plane for spiraling coefficient D=1E-3 after (a) 100, (b) 110, (c) 120, (d) 200, 300, and (e) 400 circuits.

The important footprints are shown in Fig. 6.

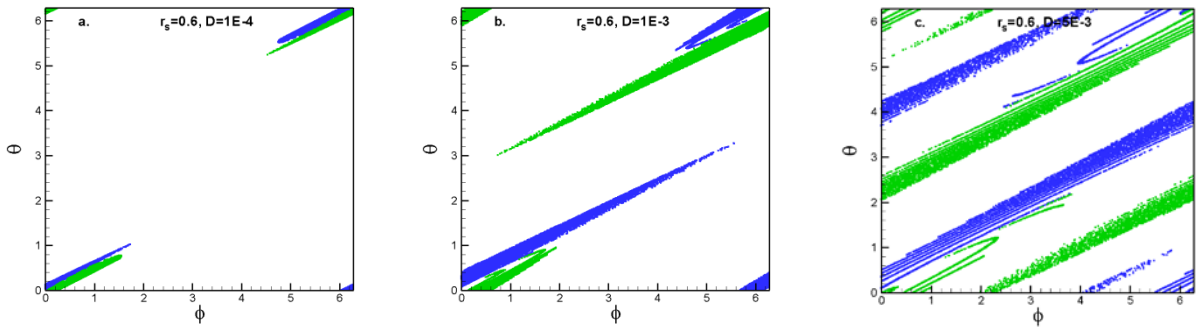

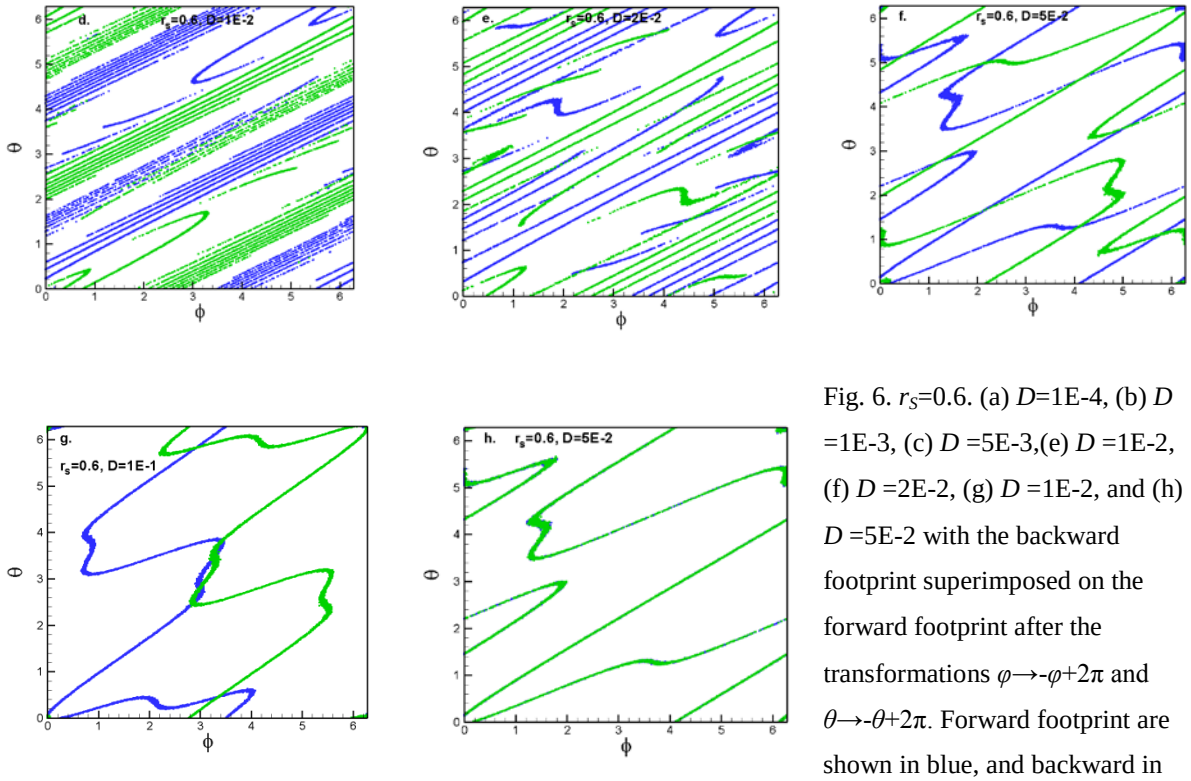

Fig. 6. r_S=0.6. (a) D=1E-4, (b) D =1E-3, (c) D =5E-3,(e) D =1E-2, (f) D =2E-2, (g) D =1E-2, and (h) D =5E-2 with the backward footprint superimposed on the forward footprint after the transformations $\varphi \rightarrow -\varphi+2\pi$ and $\theta \rightarrow -\theta+2\pi$. Forward footprint are shown in blue, and backward in green.

Generally the normalized area is larger for intercepting torus of larger radius. As D increase from 1E-5 to about 1E-2, the area increases. The rise in the area can be roughly as much as an order of magnitude. The area reaches its maximum roughly when D=1E-2. On further increase in D, the area decreases. The average length of field lines $<l>$ scales roughly as $1/D$. The average Liapunov length $<l_L>$ of the lines varies from about 50 to 5000. The slowest variation in $<l_L>$ with D is for r_S=1, and the fastest variation with D is for r_S=0.8. $<l_L>$ scales very roughly as $1/D^{1/2}$. For innermost collecting surfaces r_S=0.6, 0.7, and 0.8 the maximum e-folds do not exceed roughly 10. But for outer intercepting tori, the jump in maximum e-folds is quite large; about 24 for r_S=0.9 and about 38 for r_S=1 and 1.1. For small enough D, for these outer surfaces, e-folds can exceed 20. Large e-folds spread the heat flux on intersecting surfaces [4]. Simple models can give important results [3].

[1] Y. Feng *et al*, *Plasma Phys. Control. Fusion* **53**, 024009 (2011).

[2] N. Pomphrey *et al*, *Fusion Science and Technology* **51**, 181 (2007).

[3] A. H. Boozer, *Nuclear Fusion* **55**, 025001 (2015).

[4] A. H. Boozer, *Plasma Physics and Controlled Fusion* **52**, 104001 (2010).